Ecological Modelling 363 (2017) 111–121

Contents lists available at ScienceDirect

Ecological Modelling

journal homepage: www.elsevier.com/locate/ecolmodel

Fragment dispersal and plant-induced dieback explain irregular ring-shaped pattern formation in a clonal submerged macrophyte

Maria P. Vilas[a,*], Matthew P. Adams[b], Carolyn E. Oldham[c], Clelia L. Marti[d], Matthew R. Hipsey[a]

[a] *UWA School of Agriculture and Environment, The University of Western Australia, Crawley, Western Australia, Australia*
[b] *School of Chemical Engineering, The University of Queensland, St. Lucia, Queensland, Australia*
[c] *School of Civil, Environmental and Mining Engineering, The University of Western Australia, Crawley, Western Australia, Australia*
[d] *Sustainable Engineering Group, Faculty of Science and Engineering, Curtin University, Bentley, Western Australia, Australia*

ARTICLE INFO

Article history:
Received 25 May 2017
Received in revised form 30 August 2017
Accepted 3 September 2017

Keywords:
Potamogeton crispus
Shallow lakes
Fragment dispersal
Plant-induced dieback
Pattern formation

ABSTRACT

Submerged macrophytes can colonize shallow lakes via several reproductive mechanisms, and can in turn substantially alter these environments by modifying the thermal structure and dissolved oxygen levels within these lakes. Although multiple mechanisms of submerged macrophyte expansion have been described, the relative contribution of each of these in shallow lake environments has been largely overlooked. In this study we analyzed the spatial spread and patterning during seasonal growth of a globally invasive submerged macrophyte, *Potamogeton crispus*, in a shallow urban lake (Lake Monger, Western Australia). We used underwater and aerial imagery to estimate the spatial pattern of the *P. crispus* bed. By comparing the spatial extent of the bed at different times during the growing season, we found linear expansion rates two orders of magnitude higher than those previously estimated through rhizome elongation. We formulated a deterministic mathematical model that accounted for the ability of *P. crispus* to spread through rhizomes and fragments broken off by the feeding activities of aquatic birds, to assess the contribution of fragment dispersal to the emergent patterns of the submerged macrophyte bed. In addition to accounting for dispersal from fragments, the model also accounted for a hypothesized feedback between macrophyte-induced thermal stratification and central dieback. Comparison of our model results against field data indicated that the model accurately represented the spatial spread of the macrophyte bed when fragment dispersal was included. When fragment dispersal was not included in the model, the spatial spread of the bed was largely underestimated, suggesting that fragment dispersal may well account for the fast seasonal spread of this species. The model also captured the formation of a ring-shaped pattern in spatial macrophyte distribution suggesting that both fragment dispersal and the feedback between stratification and dieback are necessary to reproduce the spatial structure of the macrophyte bed. Our results highlight the potential important role of fragment dispersal in facilitating colonization and submerged macrophyte invasion in shallow lakes.

1. Introduction

Submerged macrophytes are fundamental components of shallow lake environments. They provide a range of ecosystem services such as nutrient retention (Boerema et al., 2014), mitigation of insecticide effects (Brogan and Relyea, 2015) and promotion of habitat heterogeneity (Kovalenko et al., 2011). They also compete with phytoplankton for nutrients and light constituting key elements of shallow lake restoration schemes (Søndergaard and Moss, 1998). Introduced invasive macrophyte species, however, tend to have fast colonization rates (Hussner et al., 2017), which can allow them to outcompete other macrophytes and establish monotypic beds. In addition, invasive submerged macrophytes tend to form dense canopies and thus reduce vertical mixing leading to bottom-water anoxia (Vilas et al., in review). Invasive macrophytes may therefore represent a threat to shallow lake ecosystems due to their potential negative impact on biodiversity and water quality (Hogsden et al., 2007). Therefore, understanding the mechanisms of invasive macrophytes expansion is of great importance both for selecting management strategies and timing their application.

The colonization success of submerged macrophytes relies on a number of factors including: a unit of dispersal and a dispersal

---

* Corresponding author.
E-mail address: maria.vilas@research.uwa.edu.au (M.P. Vilas).

http://dx.doi.org/10.1016/j.ecolmodel.2017.09.001
0304-3800/

mode (Muller-Landau, 2012), a suitable environment for successful establishment and initial growth (Riis, 2008), and suitable conditions for long-term persistence and growth (Chambers and Kalff, 1985). Submerged macrophytes can propagate into a new location through the production of seeds and vegetative propagules such as rhizomes, stolons, tubers, turions and stem fragments (Boedeltje et al., 2003; Muller-Landau, 2012). Invasive submerged macrophytes tend to take advantage of more reproductive strategies (Barrat-Segretain et al., 1998) and possess higher regeneration rates from fragments (Umetsu et al., 2012) than native species, and thus are more likely to be introduced in a new location. Once present in a new location, propagule establishment and sprouting relies on environmental factors such as the presence of propagule retention agents, light and water temperature (Riis, 2008). Long-term persistence of submerged macrophytes relies on the biophysical environment and feedbacks between the plants and their environment (van der Heide et al., 2010). It is well established that submerged macrophytes grow in areas where there is enough underwater light to support their growth (Chambers and Kalff, 1985) and where water flow is sufficiently slow to avoid uprooting, but fast enough to ensure gas and nutrient exchange (Madsen et al., 2001). In addition to the environmental conditions, submerged macrophytes interact with their environment in ways that could be positive or negative for their further development and reproduction (Maxwell et al., 2016). These feedback interactions can also play a role in determining long-term persistence of submerged aquatic vegetation (Adams et al., 2016).

Potamogeton crispus L. (curly pondweed) is an invasive submerged macrophyte that has established monotypic beds in lakes and rivers throughout the world (Bolduan et al., 1994). It behaves like a winter annual plant since it dies back in summer and regrows in autumn mainly from specialized shoot apices know as turions (Qian et al., 2015). *P. crispus* persists throughout winter and rapidly grows during spring and early summer (Catling and Dobson, 1985), when it produces seeds and turions (Chambers, 1982). During its growing season, it has the capacity to spread through both clonal propagation and stem fragments (Ganie et al., 2008), which makes it ideal for studying the relative contribution of multiple reproductive strategies to the spatial spread of invasive species. *P. crispus* is generally considered a nuisance macrophyte since it clogs waterways and alters ecosystem function and structure (Bolduan et al., 1994; Valley and Heiskary, 2012). However, in China, it is commonly used as a pioneering species when restoring degraded aquatic ecosystems (Wu et al., 2009; Zhou et al., 2016). Therefore, understanding the mechanisms contributing to *P. crispus* spatial extent is of particular relevance either to control its spread, or to effectively guide its use for restoration in degraded aquatic ecosystems.

In a recent study (Vilas et al., in review), we documented the effect of *P. crispus* on the thermal characteristics and oxygen dynamics of a shallow urban lake. We hypothesised that a negative feedback, the stratification feedback, may lead to central dieback and ring-shaped pattern formation in *P. crispus* beds that are sufficiently dense, tall and large to significantly impair vertical and lateral water transport. By obstructing water transport, the macrophytes prevent oxygenation of the bottom waters at the centre of the plant bed. This bottom-water anoxia may cause the plants in this region to experience stress due to sediment-induced anoxia (Pulido and Borum, 2010; Sand-Jensen et al., 2015) and potential toxin exposure (Borum et al., 2005), thus leading to central dieback.

Theoretical models that account for the ability of feedbacks to induce ring-shaped vegetation patterns have been developed for clonal terrestrial plants and seagrass meadows (Cartenì et al., 2012; Ruiz-Reynés et al., 2017; Sheffer et al., 2011). Most models of rings are based on scale-dependent feedbacks and were formulated to explain ring-shaped pattern formation in water-depleted environments (Sheffer et al., 2011). A model that explains ring formation in environments where water is not a limiting factor was developed by Cartenì et al. (2012). This model is based on a single negative feedback, the litter autotoxicity feedback (Mazzoleni et al., 2015, 2007), driving central dieback in clonal terrestrial grasses.

Unlike theoretical models of regular ring formation, we observed that irregular rings of spatial macrophyte distribution (Fig. 1) can form in a shallow urban lake (Lake Monger, Western Australia, Australia) (Vilas et al., in review). Irregular rings can form when clonal propagation occurs in a preferential direction (Meron et al., 2007). Submerged macrophytes have been suggested to propagate in a preferential direction in the presence of hydrodynamic forcing (Ganie et al., 2016; Puijalon et al., 2008); however, there seems to be little evidence of this mechanism occurring in lake vegetation (Wolfer and Straile, 2004). Asymmetry in the direction of seed dispersal may also have a strong influence on the appearance of vegetation patterns (Thompson and Katul, 2009). While *P. crispus* seeds are less important in the process of colonization (Rogers and Breen, 1980), fragment dispersal and regrowth from stem fragments may explain growth in a preferential direction.

Theoretical models of macrophyte expansion can be useful to assess the relative contribution of multiple dispersion mechanisms in environments where doing so is experimentally difficult. Although models that account for multiple mechanisms of dispersion have been developed for a range of populations from animals to plant pathogens (Gilligan and van den Bosch, 2008; Okubo and Levin, 2013), the use of such models to predict the spatial extent of invasive submerged macrophytes remains largely unexplored. Understanding the relative contribution of multiple mechanisms of expansion to the spatial spread of the invasive macrophyte *P. crispus* would be of value to lake managers. Therefore, we formulated a deterministic mathematical model that accounts for multiple dispersal mechanisms and a density-dependent negative feedback to address the following two questions: what are the relative contributions of fragment dispersal and clonal growth to *P. crispus* spatial spread? What are the mechanisms necessary for the formation of irregular ring-shaped patterns in shallow lake vegetation? To this end, our study first analyzes a field dataset to support model parameterization, and then uses the model to assess the above questions by comparing the predicted spatial patterns in vegetation with the field dataset.

2. Study site and field context

Lake Monger is a eutrophic shallow lake located in a heavily urbanized suburb of Perth, Western Australia (Fig. 2). It has a total surface area of 68.2 ha, a flat bottom and its mean water depth ranges from 1.21 m in spring to 0.31 m in autumn. In summer, the lake's wind climate is dominated by the sea breeze, comprised of winds blowing from the southerly, south-westerly and westerly directions (Masselink et al., 2001). Lake Monger is dominated by dense stands of the submerged macrophyte *P. crispus* during spring and summer (Leoni et al., 2016). *P. crispus* is a perennial submerged macrophyte that behaves like a winter annual (Catling and Dobson, 1985). In Lake Monger, it typically initiates growth in the middle of the lake by the beginning of spring, spreads towards the lake edges by early summer and decays after the top of the canopy reaches the water surface in mid or late summer. Ring-shaped pattern formation has been previously observed in this lake, as shown in Fig. 1.

Data used in this investigation were collected in two *P. crispus* growing seasons, 2014–2015 and 2015–2016 (Table 1). Biomass and plant height data were collected at a station located near the lake centre (LDS station, see Fig. 2). Above-ground macrophyte biomass at the LDS station was estimated by sampling a quadrat of 0.1–0.2 m^2 on the dates shown in Table 1. Plants within the quadrat

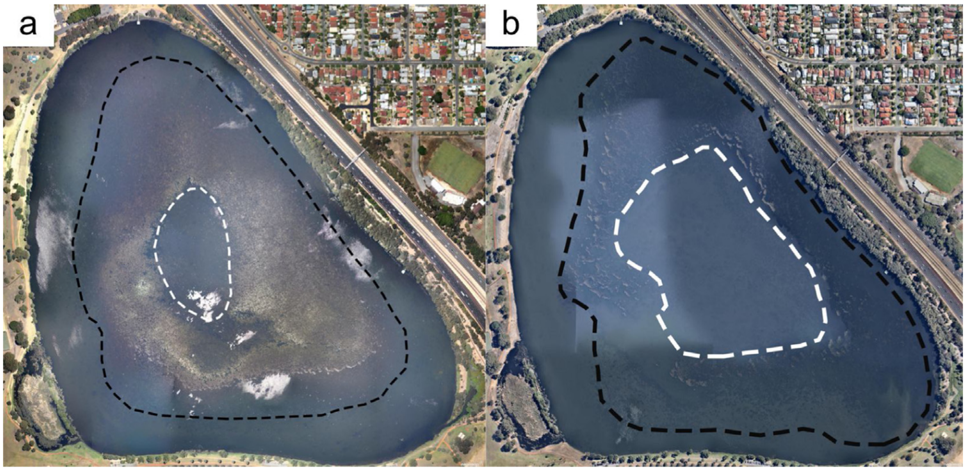

Fig. 1. Aerial image of our study site Lake Monger (Perth, Western Australia, Australia) obtained from http://maps.au.nearmap.com on 6 January 2014 (a) and 4 March 2016 (b) showing the ring-shaped pattern. The dashed black line shows the outer edge of the macrophyte bed and the dashed white line shows the inner edge of the macrophyte bed. Field surveys were not available to verify these images.

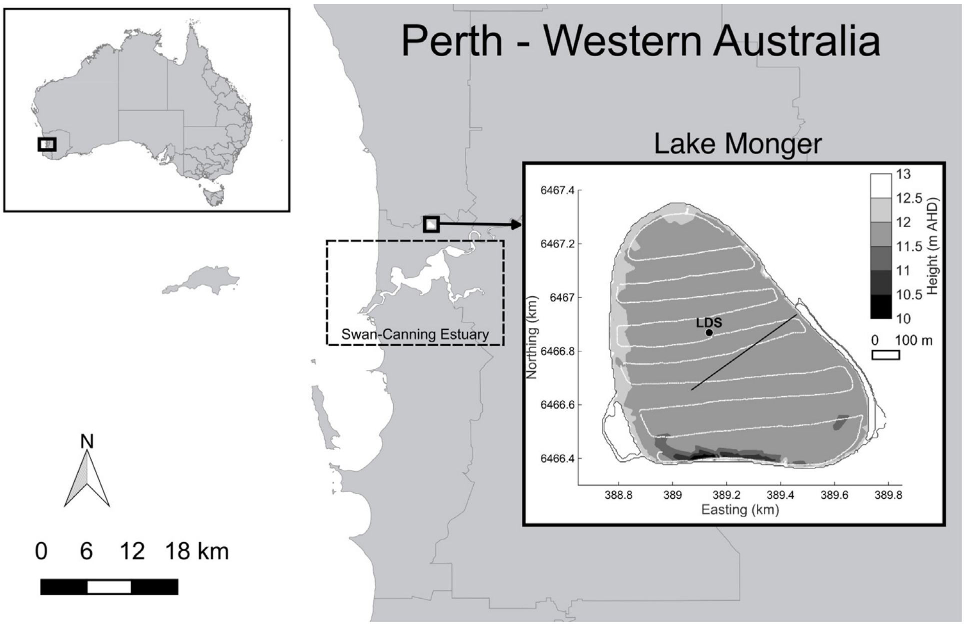

Fig. 2. Lake Monger location and bathymetry in m Australian Height Datum (AHD), showing typical transects used to identify the spatial extent of the macrophyte bed (continuous lines) and sampling station (LDS). The black line shows the transect used to estimate the linear expansion rates of the macrophyte meadow.

Table 1
Macrophyte biomass sampling dates, harvested area, number of replicates and location.

Sampling dates	Harvested area per replicate (m^2)	Number of replicates
P. crispus growing season in 2014–2015		
19 November 2014	0.2	2
2 December 2014	0.1	2
16 December 2014	0.1	2
20 January 2015	0.1	3
28 January 2015	0.1	2
8 February 2015	0.1	3
P. crispus growing season in 2015–2016		
28 October 2015	0.1	3
4 November 2015	0.1	3
23 November 2015	0.1	3
4 December 2015	0.1	3
12 January 2016	0.2	3
4 February 2016	0.2	3

were uprooted with a rake. Duplicate or triplicate biomass samples were collected and transported to the laboratory where they were washed and dried at 60 °C to a constant mass and then weighed. Canopy height was measured at randomly chosen points 5 m of the LDS station on the dates shown in Table 1. Wind speed and direction were continuously recorded in both seasons (1 October 2014–1 March 2015 and 1 October 2015–26 February 2016) by a sensor located at 2 m above the water surface at the LDS station. The sensor recorded wind speed (range: 0–75 $m\,s^{-1}$ and accuracy: 0.1 $m\,s^{-1}$) and wind direction (range: 0–360° and accuracy: 4°) data every 30 s. Wind speed at 10 m above the water surface (U_{10}) was estimated from wind speed data following the method of Verburg and Antenucci (2010).

The spatial behaviour of the macrophyte bed was inferred from limited aerial photography obtained from http://maps.au.nearmap.com (Nearmap, Dates: 27 October 2014, 8 February 2015 and 4 March 2016) in conjunction with geo-referenced movies recorded with a 10-megapixel underwater digital camera (GoPro) along

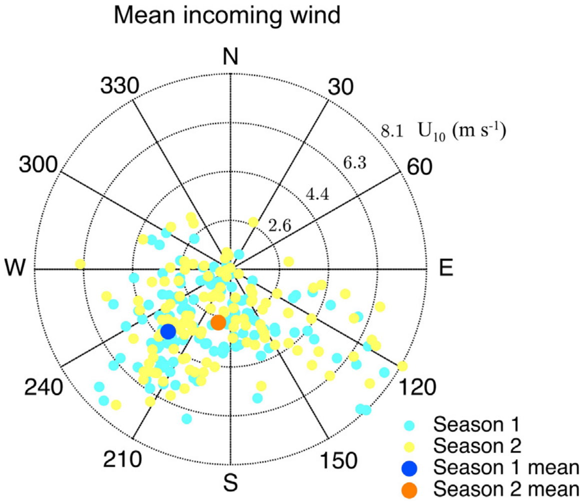

Fig. 3. Daily mean values of wind speed 10 m above the water surface (U_{10}) and direction for *P. crispus* growing season in 2014–2015 (Season 1, cyan circles) and 2015–2016 (Season 2, yellow circles). The mean values for *P. crispus* growing season in 2014–2015 (blue circle) and 2015–2016 (orange circle) are also shown.

west-east transects (Dates: 2 December 2014, 16 December 2014 and 4 November 2015) (Fig. 2). We have defined the macrophyte bed as the area in which individual plants overlapped and the sediments were mostly covered by submerged macrophytes. There was one limitation of using Nearmap images to assess the spatial pattern of the macrophyte bed: In the event of an algal bloom, the presence of plants could only be confirmed if the canopy reached the water surface. Linear expansion rates of the macrophyte bed were estimated as the slope of the linear regression line fitted to changes in the extent of the macrophyte bed over time, calculated as the distance between the bed edge and the initial bed edge on a transect perpendicular to the eastern shore of the lake (Fig. 2).

Comparison of the wind data (Fig. 3) with the macrophyte coverage data (Fig. 4) suggested that the *P. crispus* meadow expanded preferentially in the direction of the sea breeze (Fig. 3). In both growing seasons (2014–2015, Fig. 4a; and 2015–2016, Fig. 4b), the macrophytes initiated growth in the middle section of the lake and expanded mainly towards the east, northeast and southeast directions. Throughout the second growing season (2015–2016), the initial area occupied by macrophytes was larger than in the first growing season (compare Fig. 4a and b). An asymmetric ring-shaped pattern in macrophyte distribution was clearly visible by the end of the second growing season (Fig. 4b); however, central dieback also occurred around the LDS station in the first growing season (Fig. 4a and Supplementary material, Appendix D, Fig. D1).

Linear expansion rates perpendicular to the eastern shoreline for the *P. crispus* growing season in 2014–2015 were approximately $0.8 \pm 0.1\ \mathrm{m\,d^{-1}}$ in the north easterly direction and $0.3 \pm 0.1\ \mathrm{m\,d^{-1}}$ in the south westerly direction. Similarly, for the *P. crispus* growing season in 2015–2016, linear expansion rates perpendicular to the eastern shoreline were approximately $0.9\ \mathrm{m\,d^{-1}}$ in the north easterly direction and $0.6\ \mathrm{m\,d^{-1}}$ in the south westerly direction. Rhizome elongation rates in lake Potamogeton species have been estimated to range between 0.0010 and $0.0017\ \mathrm{m\,d^{-1}}$ (Kunii, 1982; Wolfer and Straile, 2004), which are two orders of magnitude lower than the linear expansion rates estimated in this study. Since rhizome elongation rates tend to decrease in nutrient rich systems (Wolfer and Straile, 2004), the use of such rates in a highly eutrophic system such as Lake Monger is justified. Therefore we can conclude that clonal expansion through rhizome elongation cannot be the primary mechanism for spatial spreading of *P. crispus* in Lake Monger.

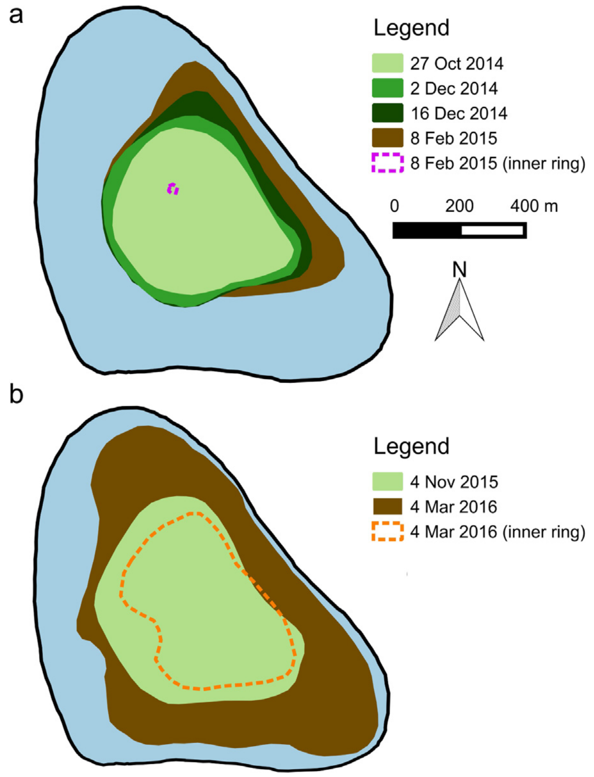

Fig. 4. Spatial extent of *P. crispus* bed on (a) 27 October 2014 (light green – http://maps.au.nearmap.com), 2 December 2014 (green – GoPro), 16 December 2014 (dark green – GoPro) and 8 February 2015 (brown – http://maps.au.nearmap.com); and (b) 4 November 2015 (light green – GoPro) and 4 March 2016 (brown – http://maps.au.nearmap.com). The pink dashed line in (a) represents the inner edge of the macrophyte bed on 8 February 2015. The orange dashed line in (b) represents the inner edge of the macrophyte bed on 4 March 2016.

The above observations were used to inform our model of macrophyte colonization, described in Section 3.

3. Model of macrophyte colonization

We present a model of *P. crispus* growth in Lake Monger, Western Australia, prior to its seasonal dieback. We did not attempt to simulate *P. crispus* sprouting or seasonal decline, only its dynamics during its growth phase, which covers approximately four months, form October to February. The model was applied to two growing seasons: 2014–2015 and 2015–2016.

3.1. Model description

The growth and colonization of the macrophyte bed was simulated using a two-dimensional advection-diffusion-reaction model. This modelling strategy has been previously used to simulate patterning in aquatic (Ruiz-Reynés et al., 2017; van der Heide et al., 2010) and terrestrial ecosystems (Tarnita et al., 2017), including regular ring formation in clonal terrestrial grasses (Cartenì et al., 2012) and fungi (Karst et al., 2016). Because the generalized dynamics of a negative feedback model giving rise to ring-shaped patterns has been investigated thoroughly elsewhere (Cartenì et al., 2012), here we focus on the application of this model type to our specific field site and our observations of macrophyte spatial patterning at this site. Based on the field observations, the model included two mechanisms for macrophyte colonization: clonal growth and vegetative dispersion of fragments, the latter of which was included because macrophyte spreading through rhizome elongation was insufficient for the rapid colonization speed identified in the field

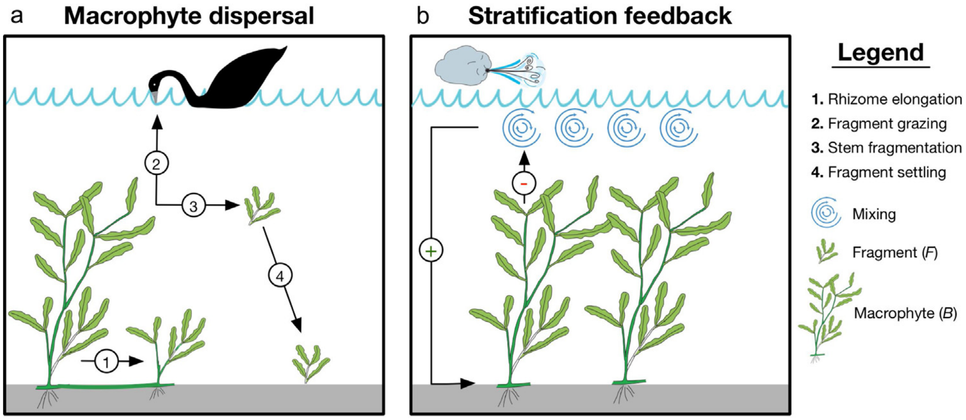

Fig. 5. Conceptual diagram of the mechanisms of macrophyte dispersal (a) and the stratification feedback (b). Mechanisms of plant dispersal in (a) are indicated with arrows (1–4). Positive and negative interactions in (b) are indicated with plus (+) and minus (−) signs respectively.

data. Since we have observed *P. crispus* fragments across the lake and since *P. crispus* can regenerate from fragments (Ganie et al., 2008), we hypothesised that fragment dispersal and regrowth from stem fragments might explain the two orders of magnitude discrepancy between the rapid spread of macrophytes observed in our system (>0.2 m–d^{-1}) and the literature estimates of *P. crispus* clonal growth (0.0010–0.0017 m–d^{-1}; Kunii, 1982; Wolfer and Straile, 2004). The model also accounts for the hypothesized feedback of macrophyte-induced stratification on central dieback, which is suggested to occur once macrophytes have occupied a sufficient height in the water column to induce low oxygen-induced stress (Vilas et al., in review). In addition, the model accounts for our observation of stronger stratification occurring at the center of the macrophyte bed (Vilas et al., in review). The interested reader is referred to Vilas et al. (in review) for an explanation of the stratification feedback. A conceptual diagram of the model is shown in Fig. 5.

The model includes three variables: macrophyte biomass B (g DW m^{-2}), macrophyte fragment mass F (g DW m^{-2}), and stratification stress S (d). Plant biomass is transferred between viable macrophytes and fragments due to breaking off of fragments from viable macrophytes (conversion of B–F) and subsequent fragment deposition onto the sediment to establish new viable macrophytes (conversion of F–B). Since Lake Monger hosts hundreds of black swans (*Cygnus atratus*) during the spring and summer (Anonymous, 2007), fragment production is assumed to occur during the feeding activities of black swans. Strong winds could also enhance propagule abscission (Thompson and Katul, 2013); however, the contribution of this mechanism to fragments breaking off in a low energy environment such as Lake Monger is likely to be minimal. The black swan population is assumed to remain constant during the growing season of the macrophyte, thus the rate of fragment production is assumed constant in time. Fragments are also assumed to be removed from the lake due to grazing by swans (Mitchell et al., 1988). The stratification stress S can be physically interpreted as the total time that the macrophytes well within the meadow have been stressed due to the presence of locally stratified waters, without being specific as to whether this stress is due to anoxia or sulphide accumulation in the sediment.

Macrophytes, with biomass B (g DW m^{-2}), are assumed to grow logistically, break into fragments, spatially colonize the lake through rhizome elongation and deposition of viable fragments, and decline when sufficiently stressed by thermal stratification, so that:

$$\frac{\partial B}{\partial t} = D_B\nabla^2 B + \mu B\left(1-\frac{B}{B_{max}}\right) + rF - gB - m_B H(S-S_{th})H(B), \quad (1)$$

where the constant diffusion coefficient $D_B = \frac{v^2}{4\mu}$ (Holmes et al., 1994) represents macrophyte expansion due to rhizome elongation in terms of the spreading speed v (m d^{-1}), μ is the maximum macrophyte growth rate (d^{-1}), $\nabla^2 = \frac{\partial^2}{\partial x^2} + \frac{\partial^2}{\partial y^2}$ is the Laplacian operator, $B_{\max}$ is the macrophyte maximum biomass supported by the system (carrying capacity, in g DW m^{-2}), r is the rate of fragment conversion to viable macrophytes (d^{-1}), g is the rate of macrophyte conversion to fragments (d^{-1}), m_B is the mortality rate due to stratification stress (g DW m^{-2} d^{-1}), $H(x)$ are Heaviside step functions, and S_{th} is the critical value of stratification stress above which plants decline (d). Stratification stress-induced mortality only occurs when (1) there is non-zero biomass and (2) the stratification stress S exceeds the critical value S_{th} required for this stress to induce mortality; these two requirements were both implemented in the model using Heaviside step functions. Mortality is assumed to be linear in time (Collier et al., 2016) and can therefore be approximated by $m_B = \frac{B_{max}}{t_m}$, where t_m is the time to mortality due to stratification stress (d).

Viable fragments, with biomass F (g DW m^{-2}), are assumed to disperse horizontally throughout the lake and advect preferentially in the direction of the prevailing wind, be produced by breaking off of viable macrophyte biomass, be deposited in the sediment, and be lost due to swan herbivory, so that:

$$\frac{\partial F}{\partial t} + \nabla.(f_B(B)\mathbf{a}F) = \nabla.(f_B(B)D_F\nabla F) + gB - rF - m_F F. \quad (2)$$

where $f_B(B) = \left(1-\frac{B}{B_{max}}\right)$ is the factor reduction in lateral advection and dispersion of fragments due to viable macrophyte presence (no units), **a** is the velocity of stem fragments due to wind-induced advection when no macrophytes are present (m d^{-1}), D_F is the diffusion coefficient of stem fragments when no macrophytes are present (m^2 d^{-1}), and m_F is the mortality rate of fragments due to herbivory (d^{-1}). The factor $f_B(B)$ reduces fragment transport with increasing macrophyte biomass, to account for fragment capture and retention by the existing macrophyte biomass (Riis and Sand-Jensen, 2006). Fragment settling is assumed to be analogous to the sinking velocity of suspended particles and thus assumed proportional to macrophyte biomass (Cerco and Moore, 2001). The justification for this assumption is that submerged macrophytes reduce flow velocities (Leonard and Croft, 2006) and therefore allow for fragment settling. Although this is a simplified representation of fragment settling it is likely to be an appropriate approximation in dense canopies such as those commonly established by *P. crispus*. Any violation of this assumption would imply that the fragments do not settle in the presence of macrophyte

Table 2
Summary of the model equations. The model variables and parameters are defined in Table 3.

$$\frac{\partial B}{\partial t} = \frac{\nu^2}{4\mu}\nabla^2 B + \mu B\left(1 - \frac{B}{B_{max}}\right) + rF - gB - \frac{B_{\max}}{t_m}H(S - S_{th})H(B) \quad (4)$$

$$\frac{\partial F}{\partial t} + \nabla.\left(\left(1 - \frac{B}{B_{\max}}\right)\beta\sqrt{\frac{C_D\rho_a}{\rho_w}}\boldsymbol{U}_{10}F\right) = \nabla.\left(\left(1 - \frac{B}{B_{\max}}\right)D_F\nabla F\right) + gB - rF - m_F F \quad (5)$$

$$\frac{dS}{dt} = min\left(\frac{L}{L_{st}}, 1\right)H\left(\frac{B}{\alpha} - h_{crit}\right) \quad (6)$$

biomass and thus that the model would underestimate the extent of fragment transport.

Fragments were observed to float at different depths in the field, and fragments near the water surface will be advected more by the wind than fragments near the lake bottom. Therefore, we assumed that the depth-averaged velocity of fragments due to wind advection is proportional to, and less than, the surface water velocity. We treated the surface shear velocity $\mathbf{u}^*$ ($\mathrm{m\,d^{-1}}$) as a proxy for the surface water velocity (Amorocho and DeVries, 1980), to obtain $\mathbf{a} = \beta\mathbf{u}^*$, where the ratio of fragment velocity to surface shear velocity β (no units) must be less than unity to account for the different water depths at which fragments float. The surface shear velocity can be calculated as $\mathbf{u}* = \sqrt{\frac{C_D\rho_a}{\rho_w}}\mathbf{U_{10}}$, where C_D is the wind drag coefficient (no units), ρ_a and ρ_w are the densities of air and water respectively ($\mathrm{kg\,m^{-3}}$), and U_{10} is the wind speed at 10 m height ($\mathrm{m\,d^{-1}}$).

Based on the results of our previous study we assumed that the macrophytes accumulate local stress S after they induce thermal stratification of the water column. In previous experimental work (Vilas et al., in review), we identified that (1) stratification is induced only once macrophytes exceed a critical height threshold (at least 50% of the water column), and (2) stratification is strongest at the centre of the bed compared with the bed edges. Following on from the second observation, we assumed that the stratification stress on macrophytes depends on the distance L (m) to the nearest meadow edge, and this stress is maximal when L exceeds a threshold length scale L_{st} (m) the value of which was estimated as O(100 m) in our previous study. Combining these considerations, we defined a trapezoidal kernel for stratification stress S, for areas colonized by macrophytes, as

$$\frac{dS}{dt} = \begin{cases} \min\left(\frac{L}{L_{st}}, 1\right), & h \geq h_{crit}, \\ 0, & h < h_{crit}, \end{cases} \quad (3)$$

where h is the canopy height as a fraction of the local water depth (no units), h_{crit} is the critical value of h above which thermal stratification develops (at least 50% of the water column, therefore $h_{crit} = 0.5$), L is the distance to the nearest macrophyte meadow edge (m), and L_{st} is the minimum distance from the bed edge above which the stress on macrophytes due to thermal stratification is maximal (m). We found that the relationship between macrophyte biomass B ($\mathrm{g\,DW\,m^{-2}}$) and relative canopy height h was linear (adjusted $R^2 \geq 0.9$ for both growing seasons, see Supplementary material, Appendix A, Fig. A2), and therefore we estimated the canopy relative height as $h = B/\alpha$, where α is the ratio of biomass to canopy relative height ($\mathrm{g\,DW\,m^{-2}}$).

3.2. Model setup and simulations

The full model equations are shown in Table 2, and model parameters are shown in Table 3 and justified in Appendix A. Where possible parameters were obtained from this study, otherwise they were taken from literature values, or estimated to better represent the observed patterns of *P. crispus* growth and expansion. The model was solved numerically using the explicit Euler method, with diffusion and advection terms discretised using second order central difference and first order upwinding schemes, respectively.

We ran three different simulations: (1) the first growing season (2014–2015) excluding fragment dispersal ($r = 0$, $F = 0$), (2) the first growing season (2014–2015) including fragment dispersal ($r > 0$), and (3) the second growing season (2015–2016) including fragment dispersal ($r > 0$). The two simulations for the first growing season were initialised to match a starting date of 27 October 2014, with macrophyte biomass B occupying the full spatial extent of the meadow observed on that day (Fig. 4a). The initial macrophyte biomass within the meadow was assumed to be 12 $\mathrm{g\,DW\,m^{-2}}$, as this biomass value is predicted on 27 October 2014 from fitting a logistic curve to data for macrophyte biomass versus time measured at the LDS station (Supplementary material, Appendix A, Fig. A1a). Simulations for the first growing season were run for 104 days. The simulation for the second growing season was initialised to match a starting date of 4 November 2015, similarly with an initial macrophyte biomass occupying the full spatial extent of the meadow observed on that day (Fig. 4b) and equal to 20 $\mathrm{g\,DW\,m^{-2}}$ from fitting a logistic curve to data for biomass versus time at the LDS station (Supplementary material, Appendix A, Fig. A1b). This simulation was run for 114 days. In simulations where fragment dispersal was included, the fragments F were assumed to occupy the same initial spatial extent as the macrophytes B, with the same initial biomass (i.e., $F = 12\,\mathrm{g\,DW\,m^{-2}}$ on 27 October 2014, and $F = 20\,\mathrm{g\,DW\,m^{-2}}$ on 4 November 2015). Zero-flux boundary conditions were assumed at the edges of the lake. The lake covers a total area of 68.2 ha, and was discretised onto a two-dimensional grid consisting of square cells of 2.5 m × 2.5 m size, and a time step of 0.0025 d. To ensure our numerical discretization was appropriate, we ran additional simulations with reduced time step (0.00025 d) and reduced cell size (1 m × 1 m); our model results were negligibly affected by these changes in discretization (data not shown).

3.3. Comparison with hydrodynamic simulations

Our advection-diffusion-reaction model for macrophyte colonization, equations (4)–(6), approximates the fragment transport throughout the lake via simple advection and diffusion terms that, while computationally efficient, will not be as accurate as a hydrodynamic model. However, the coupling of a two- or three-dimensional, temporally-changing, plant growth model to an equivalent hydrodynamic model is technically more challenging and was beyond the scope of this work. To resolve any discrepancies between our model's approximation of fragment transport, and the fragment transport predicted by a hydrodynamic model, we used the 3D Estuary, Lake and Coastal Ocean Model (ELCOM, Hodges et al., 2000) to identify water transport patterns through a static submerged macrophyte meadow occupying the same spatial extent as observed in Lake Monger in late summer of 2015 (Supplementary material, Appendix D, Fig. D1). Specifically, an evenly distributed conservative numerical tracer was released everywhere within the macrophyte meadow for 10 h on 28 January 2015 between 10:00 and 20:00 h, to identify the pattern of water motion in the lake. This date was chosen because the wind conditions were dominated by the sea breeze components.

Table 3
Model parameters, description, values, units and source. S1 stands for *P. crispus* growing season in 2014–2015 and S2 stands for *P. crispus* growing season in 2015–2016.

	Description	Values		Units	Source
		S1	S2		
Variable					
B	Macrophyte biomass			$\mathrm{g\,DW\,m^{-2}}$	
F	Fragment biomass			$\mathrm{g\,DW\,m^{-2}}$	
h	Macrophyte height relative to water depth			–	
L	Distance to the nearest meadow edge			m	
S	Stratification stress			d	
U_{10}	Wind speed at 10 m height			$\mathrm{m\,s^{-1}}$	Our study
Parameter					
$B_{\max}$	Plant biomass carrying capacity	470	200	$\mathrm{g\,DW\,m^{-2}}$	Our study
C_D	Drag coefficient	0.0013	0.0013	–	Amorocho and DeVries (1980)
D_F	Diffusion coefficient of fragments	100	100	$\mathrm{m^2\,d^{-1}}$	Murphy et al. (2007)
g	Biomass to fragments conversion rate	0.007	0.007	$\mathrm{d^{-1}}$	Estimated
h_{crit}	Critical canopy height for stratification	0.5	0.5	–	Our study
L_{st}	Stratification length scale	100	100	m	Our study and Bartleson (2004)
m_F	Fragments mortality rate	0.05	0.05	$\mathrm{d^{-1}}$	Estimated
r	Fragments to biomass conversion rate	0.1	0.1	$\mathrm{d^{-1}}$	Estimated
S_{th}	Time required for stress to induce mortality	50	50	d	Our study
t_m	Time to mortality	5	5	d	Sand-Jensen et al. (2015)
v	Rhizome elongation speed	0.0017	0.0017	$\mathrm{m\,d^{-1}}$	Wolfer and Straile 2004
α	Biomass to relative height ratio	470	200	$\mathrm{g\,DW\,m^{-2}}$	Our study
β	Ratio of fragment velocity to shear velocity	0.02	0.02	–	Estimated
μ	Maximum growth rate	0.07	0.07	$\mathrm{d^{-1}}$	Our study
ρ_a	Air density	1.2	1.2	$\mathrm{kg\,m^{-3}}$	
ρ_w	Water density	1000	1000	$\mathrm{kg\,m^{-3}}$	

4. Results

4.1. Clonal propagation versus fragment dispersal

The model adequately represented the spatial pattern of *P. crispus* growth and expansion when fragment dispersal was included (Fig. 6e–h). In contrast, when fragment dispersal was excluded from the model, the spatial spread of the macrophyte bed was largely underpredicted (Fig. 6a–d). On 8 February 2015 the model showed a slightly greater macrophyte spread compared with the field estimations. It is worth noting that on 8 February 2015, the lake took a green colour (Supplementary material, Appendix D, Fig. D1), which complicated the mapping of the macrophyte bed edge. This likely resulted in an underestimation of the spatial extent of the bed, since the presence of macrophytes could only be confirmed if the plants reached the water surface. As for the simulated *P. crispus* fragments, they expanded towards the easterly directions and largely remained within the macrophyte bed (Fig. 6i–l).

4.2. Irregular ring-shaped pattern formation

In the *P. crispus* growing season in 2015–2016 central dieback was clearly observed in the field data, and our model's prediction of the spatial extent of the inner ring was in good agreement with the field observations (Fig. 7d, Supplementary material, Video 1). The simulated fragments largely remained within the macrophyte bed (Fig. 7e–h) and the area of the macrophyte bed exposed to stratification increased as the plants expanded outwards (Fig. 7i–l).

Simulations run for *P. crispus* growing season in 2014–2015 including fragment dispersal, predicted a decline in macrophyte biomass at the LDS station on 9 February 2015. In the field, central loss at the LDS station was evident on 8 February 2015 (Fig. 8 and Supplementary material, Appendix D, Fig. D1), yielding only a 1 day difference between the predicted mortality date by the model and the field data. Simulations runs for *P. crispus* growing season in 2015–2016, predicted no biomass at the LDS station on 26 January 2016; this agrees with our observations of no biomass at the LDS station on 4 February 2016 and water temperature data showing that bottom and top waters fully mixed after 25 January 2016 (Fig. 8 and Supplementary material, Appendix C). It is worth noting that *P. crispus* biomass in the second growing season (2015–2016) was half that of the previous growing season; thus, our chosen value for the critical canopy height beyond which thermal stratification may occur ($h_{crit} = 0.5$) may underestimate the real value for the second growing season. To account for potential differences in the critical canopy height, we ran additional model simulations with $h_{crit} = 0.6$ and $h_{crit} = 0.8$, and found only small differences in the spatial extent of the inner ring (Supplementary material, Appendix B, Fig. B1).

Overall, the model accurately represented the measured biomass at the LDS station and the spatial pattern of the macrophyte bed, suggesting a good fit of our model to the field data. The model slightly underpredicted the macrophyte spread towards the southerly directions in the *P. crispus* growing season in 2015–2016 (Fig. 7a–d).

4.3. Comparison with hydrodynamic simulations

Three-dimensional simulations of tracer concentrations carried out with the hydrodynamic model ELCOM on a typical summer day with sea breeze indicated that particle transport was largely influenced by the direction of the wind (Fig. 9). At 12:00 h the tracer remained within the macrophyte bed. As the day progressed, the tracer was transported in the direction of the wind (Fig. 9a–d). When it reached the eastern boundary of the lake, it was preferentially transported towards the southern area of the lake (Fig. 9d), suggesting that the use of a hydrodynamic model coupled to our advection-diffusion-reaction model will likely resolve the discrepancy between our model and field data.

5. Discussion

This study used a spatially explicit model to demonstrate that (a) macrophyte colonization via fragment dispersal and (b) plant-induced dieback are likely to be the primary mechanisms controlling the spatial and temporal dynamics of the seasonal growth of an invasive macrophyte present in a highly urbanised lake (*P. crispus* in Lake Monger, Perth, Australia). Although substantial research has suggested that fragment dispersal and

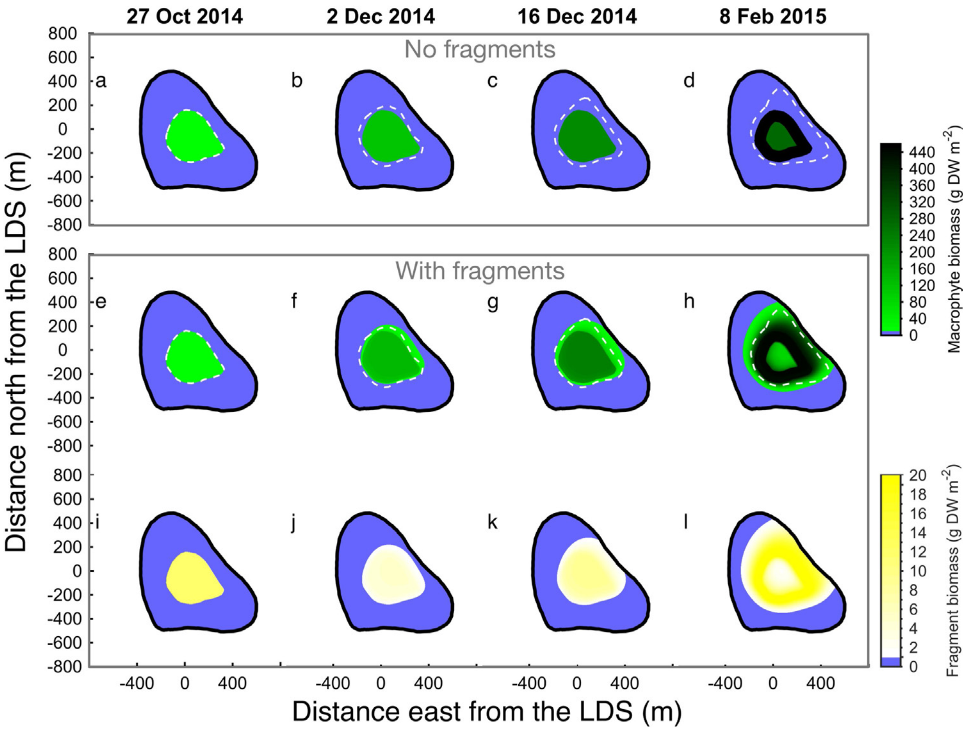

Fig. 6. Simulated macrophyte biomass on 27 October 2014 (initial condition) (a), 2 December 2014 (b), 16 December 2014 (c) and 8 February 2014 (d) without fragment dispersal. Simulated macrophyte biomass on 27 October 2014 (e), 2 December 2014 (f), 16 December 2014 (g) and 8 February 2014 (h) with fragment dispersal. Simulated fragment biomass on 27 October 2014 (i), 2 December 2014 (j), 16 December 2014 (k) and 8 February 2014 (l) with fragment dispersal. The white dashed line indicates the extent of the macrophyte bed estimated from Nearmap images (27 October 2014 and 8 February 2015) or underwater images (2 December 2014 and 16 December 2014).

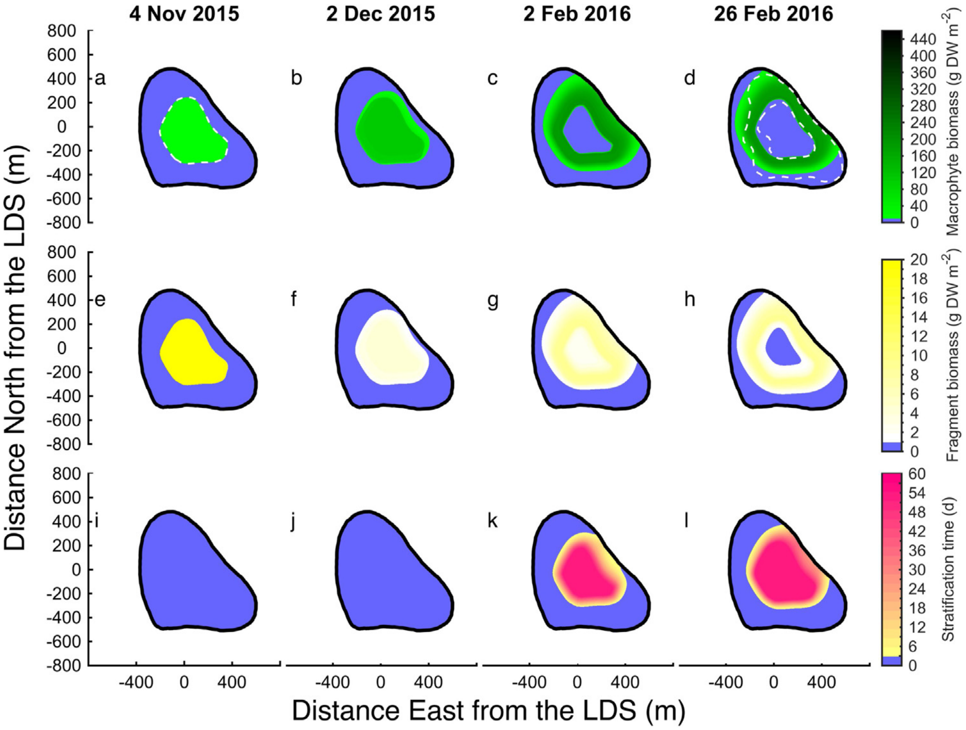

Fig. 7. Simulated macrophyte biomass on 4 November 2015 (initial condition) (a), 2 December 2015 (b), 2 February 2016 (c) and 26 February 2016 (d) with fragment dispersal. Simulated fragment biomass on 4 November 2015 (e), 2 December 2015 (f), 2 February 2016 (g) and 26 February 2016 (h). Simulated stratification time on 4 November 2015 (i), 2 December 2014 (j), 2 February 2016 (k) and 26 February 2016 (l). The white dashed line indicates the extent of the macrophyte bed estimated from Nearmap images (4 March 2016) or underwater images (4 November 2015).

regeneration from stem fragments are important contributors to the survival and spatial spread of aquatic vegetation (Barrat-Segretain et al., 1998; Vári, 2013), these processes are rarely taken into account when modelling the spatial extent of aquatic vege-

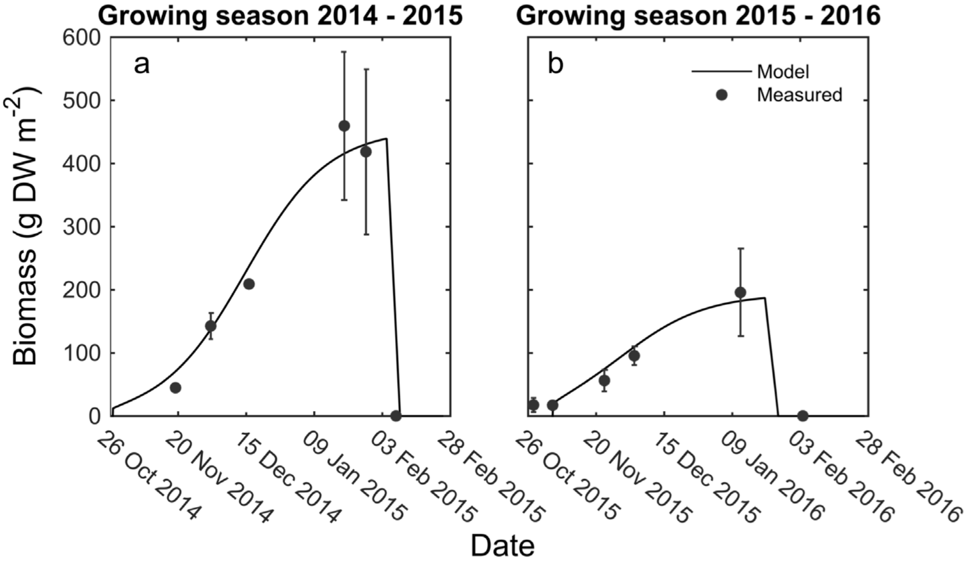

Fig. 8. (a) *P. crispus* mean biomass at the LDS station (black circles) and standard deviation (black error bars) for *P. crispus* growing season in 2014–2015 and simulated biomass at the LDS station when fragment dispersal is included in the model (black line). (b) *P. crispus* mean biomass at the LDS station (black circles) and standard deviation (black error bars) for *P. crispus* growing season in 2015–2016 and simulated biomass at the LDS station when fragment dispersal is included in the model (black line).

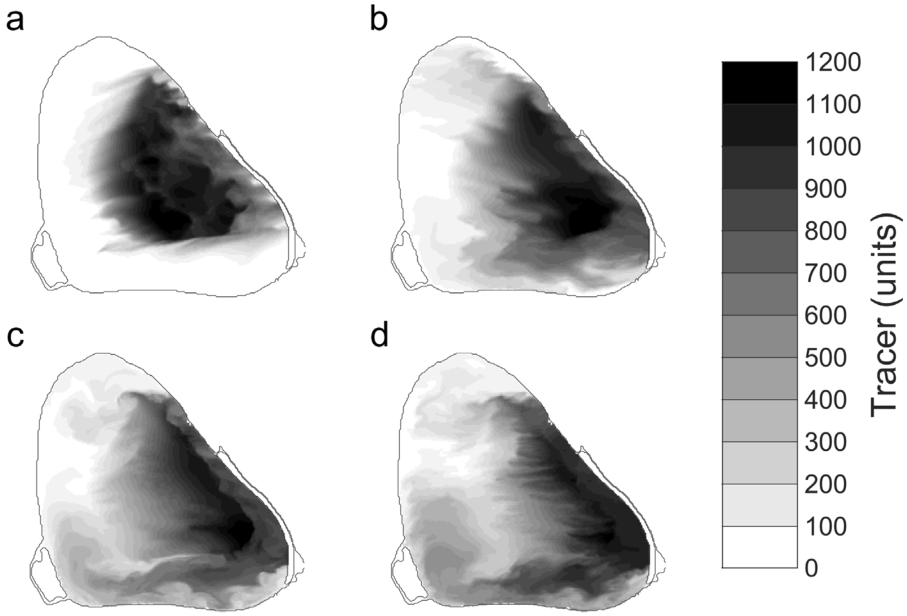

Fig. 9. Depth-averaged numerical tracer concentration on 28 January 2015 at 12:00 h (a), 16:00 h (b), 20:00 h (c) 24:00 h (d) for a simulated canopy height relative to water depth of 0.1. The tracer is released from all depths within the macrophyte bed at a rate of 1 unit per 30 s for all times between 10:00 h and 20:00 h.

tation. For instance, previous studies on seagrass dispersal were based on hydrodynamic models only of seed dispersal (Grech et al., 2016; Ruiz-Montoya et al., 2015). A model that accounts for macrophyte propagule dispersal (including fragments) has been developed for wetland ecosystems (Ursino, 2010); however, this model uses a diffusion-based approach that neglects the potential asymmetry in the direction of fragment dispersal that may emerge if water flows in a preferential direction. Models developed for arid plant communities that use advection-diffusion-based approaches to account for seed dispersal, have suggested that diffusion-based models fail to represent the important features of propagule dispersal (Thompson and Katul, 2009). We provide support to those suggestions by showing that fragment dispersal and wind-induced advection of stem fragments may have a strong influence on the spatial spread of macrophyte beds.

Simulations runs for the *P. crispus* growing season in 2014–2015 showed that when fragment dispersal was set to zero, the spatial extent of the macrophyte bed was largely underestimated (Fig. 6). Conversely, the incorporation of fragment dispersal and regrowth from stem fragments into the model resulted in an adequate representation of the spatial spread of the macrophyte bed, suggesting that *P. crispus* may rely widely on fragment dispersal to spatially colonize a habitat. Simulations run for the *P. crispus* growing season in 2015–2016 indicate that the model underpredicted the spatial extent of the macrophyte bed, particularly towards the southern area of the lake. Tracer simulations using a hydrodynamic model showed that on a typical day with sea breeze, the flow diverted preferentially towards the south-eastern boundary of the lake (see Fig. 8), indicating that the use of a hydrodynamic model is likely to better resolve the spread towards this region. Embedding this model into a hydrodynamic model was beyond the scope of this study; however, we suggest that this is a necessary step towards predicting the spatial spread of *P. crispus* in Lake Monger and other shallow lake ecosystems.

Our field data also supported our suggestions that *P. crispus* may rely on fragment dispersal to spatially colonize a habitat. Linear expansion rates of *P. crispus* were two orders of magnitude higher than those estimated solely through rhizome elongation (Kunii, 1982; Wolfer and Straile, 2004), suggesting that fragment dispersal may account for the rapid spread of this species. This is supported by previous studies suggesting that multiple reproductive strategies potentially contribute to the invasiveness of *P. crispus* (Ganie et al., 2008). Although seed and turion banks could also have played a role in explaining the fast spread of *P. crispus*, previous studies indicate that *P. crispus* seeds rarely geminate (Rogers and Breen, 1980), and turions usually undergo summer dormancy (Sastroutomo, 1981). This further supports our hypothesis that stem fragmentation may well explain the fast spread of this species. Fragment dispersal may also account for the rapid colonization potential of other invasive species (Ganie et al., 2016). For instance, high regeneration rates have been estimated for *Elodea canadensis* (Barrat-Segretain et al., 1998) and *Myriophyllum spicatum* L. (Riis et al., 2009). While colonization through fragment dispersal is a recurrent trait in invasive macrophyte species (Vári, 2013), some submerged macrophytes rarely propagate through fragment dispersal (Barrat-Segretain et al., 1998; Riis, 2008). Hence, whether fragment dispersal is an important component of macrophyte invasion is still highly debated. Recent work has suggested that invasive species do not possess higher rates of breakage than native plants (Heidbüchel et al., 2016). The model presented here may therefore be useful to investigate the role of fragment dispersal on the invasiveness of aquatic plant species.

Overall, our study suggests that the overlooked dynamics of fragment dispersal and survival may have a strong influence on the spatial patterns of aquatic vegetation. Therefore, detailed field studies of fragment dispersal are a clear next research step, in order to better represent this process in future model parameterizations. The model results also support our hypothesis that macrophyte-induced thermal stratification may well lead to ring-shaped pattern formation (Vilas et al., in review). Simulations runs for *P. crispus* growing season in 2015–2016 showed that the model accurately predicted the extent of the ring and the time of central dieback and may therefore be useful to simulate central dieback in other submerged macrophytes. Previous models of ring formation were developed to account for regular ring formation (Cartenì et al., 2012; Karst et al., 2016; Ruiz-Reynés et al., 2017). Here we expand upon those frameworks to consider irregular rings and by providing a mortality term, which yields a finite time until macrophyte death. This mortality term is appropriate for ecosystems where concentric rings do not occur. We also provide additional evidence for a specific mechanism of plant dieback due to demographic imbalance (Ruiz-Reynés et al., 2017). Further research into the biogeochemical processes involved in the stratification feedback is required to better represent it in future model parameterizations.

6. Conclusions

The results of this investigation suggest that plant fragment dispersal is likely a key mechanism that potentially explains the fast spread of the submerged macrophyte *Potamogeton crispus*. Macrophyte fragment dispersal and regeneration from stem fragments are overlooked mechanisms when restoring degraded ecosystems or managing invasive species. We demonstrated how these processes can be incorporated in the modelling of aquatic vegetation in shallow lakes. This is a necessary step to predict the spatial spread and patterning of submerged vegetation in this and other aquatic ecosystems.

Acknowledgments

The authors thank Brodie A. J. Lawson for helpful discussions during model development. Gregory Attwater is thanked for his support on the acquisition of field data. Maria P. Vilas also acknowledges the Town of Cambridge, Centre for Water Research and SIRF scholarships. Clelia L. Marti was the recipient of the “Lake Monger – understanding of its functioning” project financed by the Town of Cambridge. Matthew R. Hipsey received funding from the Australian Research Council (LP130100756).

Appendix A. Supplementary data

Supplementary data associated with this article can be found, in the online version, at http://dx.doi.org/10.1016/j.ecolmodel.2017.09.001.

References

Adams, M.P., Hovey, R.K., Hipsey, M.R., Bruce, L.C., Ghisalberti, M., Lowe, R.J., Gruber, R.K., Ruiz-Montoya, L., Maxwell, P.S., Callaghan, D.P., Kendrick, G.A., O’Brien, K.R., 2016. Feedback between sediment and light for seagrass: where is it important? Limnol. Oceanogr. 61, 1937–1955, http://dx.doi.org/10.1002/lno.10319.

Amorocho, J., DeVries, J.J., 1980. A new evaluation of the wind stress coefficient over water surfaces. J. Geophys. Res. 85, 433, http://dx.doi.org/10.1029/JC085iC01p00433.

Anonymous, 2007. Lake Monger Reserve Management Plan 2008–2018. Floreat, Western Australia.

Barrat-Segretain, M.-H., Bornette, G., Hering-Vilas-Bôas, A., 1998. Comparative abilities of vegetative regeneration among aquatic plants growing in disturbed habitats. Aquat. Bot. 60, 201–211, http://dx.doi.org/10.1016/S0304-3770(97)00091-0.

Bartleson, R.D., 2004. Interactions of Seagrass Beds and the Water Column: Effects of Bed Size and Hydrodynamics. University of Maryland, Ph.D. thesis http://drum.lib.umd.edu/handle/1903/2106.

Boedeltje, G., Bakker, J.P., Bekker, R.M., van Groenendael, J.M., Soesbergen, M., 2003. Plant dispersal in a lowland stream in relation to occurrence and three specific life-history traits of the species in the species pool. J. Ecol. 91, 855–866, http://dx.doi.org/10.1046/j.1365-2745.2003.00820.x.

Boerema, A., Schoelynck, J., Bal, K., Vrebos, D., Jacobs, S., Staes, J., Meire, P., 2014. Economic valuation of ecosystem services, a case study for aquatic vegetation removal in the Nete catchment (Belgium). Ecosyst. Serv. 7, 46–56, http://dx.doi.org/10.1016/j.ecoser.2013.08.001.

Bolduan, B.R., Van Eeckhout, G.C., Quade, H.W., Gannon, J.E., 1994. Potamogeton crispus–the other invader. Lake Reserv. Manag. 10, 113–125, http://dx.doi.org/10.1080/07438149409354182.

Borum, J., Pedersen, O., Greve, T.M., Frankovich, T.A., Zieman, J.C., Fourqurean, J.W., Madden, C.J., 2005. The potential role of plant oxygen and sulphide dynamics in die-off events of the tropical seagrass, *Thalassia testudinum*. J. Ecol. 93, 148–158, http://dx.doi.org/10.1111/j.1365-2745.2004.00943. x.

Brogan, W.R., Relyea, R.A., 2015. Submerged macrophytes mitigate direct and indirect insecticide effects in freshwater communities. PLoS One 10, e0126677, http://dx.doi.org/10.1371/journal.pone.0126677.

Cartenì, F., Marasco, A., Bonanomi, G., Mazzoleni, S., Rietkerk, M., Giannino, F., 2012. Negative plant soil feedback explaining ring formation in clonal plants. J. Theor. Biol. 313, 153–161, http://dx.doi.org/10.1016/j.jtbi.2012.08.008.

Catling, P.M., Dobson, I., 1985. The biology of Canadian weeds: 69. *Potamogeton crispus* L. Can. J. Plant Sci. 65, 655–668, http://dx.doi.org/10.4141/cjps85-088.

Cerco, C.F., Moore, K., 2001. System-wide submerged aquatic vegetation model for chesapeake bay. Estuaries 24, 522, http://dx.doi.org/10.2307/1353254.

Chambers, P.A., Kalff, J., 1985. The influence of sediment composition and irradiance on the growth and morphology of *Myriophyllum spicatum* L. Aquat. Bot. 22, 253–263, http://dx.doi.org/10.1016/0304-3770(85)90003-8.

Chambers, P.A., 1982. Light, Temperature and the Induction of Dormancy in Potamogeton Crispus and Potamogeton Obtusifolius. University of St. Andrews (Ph.D. thesis).

Collier, C.J., Adams, M.P., Langlois, L., Waycott, M., O’Brien, K.R., Maxwell, P.S., McKenzie, L., 2016. Thresholds for morphological response to light reduction for four tropical seagrass species. Ecol. Indic. 67, 358–366, http://dx.doi.org/10.1016/j.ecolind.2016.02.050.

Ganie, A.H., Reshi, Z., Wafai, B.A., 2008. Multiple reproductive strategies contribute to invasiveness of *Potamogeton Crispus* L. (Potamogetonaceae) in freshwater ecosystems of Kashmir Himalaya, India. Proceedings of Taal 2007: The 12th World Lake Conference, 1067–1073.

Ganie, A.H., Reshi, Z.A., Wafai, B.A., Puijalon, S., 2016. Clonal growth architecture and spatial dynamics of 10 species of the genus *Potamogeton* across different habitats in Kashmir Valley, India. Hydrobiologia 767, 289–299, http://dx.doi.org/10.1007/s10750-015-2509-5.

Gilligan, C.A., van den Bosch, F., 2008. Epidemiological models for invasion and persistence of pathogens. Annu. Rev. Phytopathol. 46, 385–418, http://dx.doi.org/10.1146/annurev.phyto.45.062806.094357.

Grech, A., Wolter, J., Coles, R., McKenzie, L., Rasheed, M., Thomas, C., Waycott, M., Hanert, E., 2016. Spatial patterns of seagrass dispersal and settlement. Divers. Distrib. 22, 1150–1162, http://dx.doi.org/10.1111/ddi.12479.

Heidbüchel, P., Kuntz, K., Hussner, A., 2016. Alien aquatic plants do not have higher fragmentation rates than native species: a field study from the River Erft. Aquat. Sci. 78, 767–777, http://dx.doi.org/10.1007/s00027-016-0468-1.

Hodges, B.R., Imberger, J., Saggio, A., Winters, K.B., 2000. Modeling basin-scale internal waves in a stratified lake. Limnol. Oceanogr. 45, 1603–1620, http://dx.doi.org/10.4319/lo.2000.45.7.1603.

Hogsden, K.L., Sager, E.P.S., Hutchinson, T.C., 2007. The Impacts of the non-native macrophyte *Cabomba caroliniana* on littoral biota of Kasshabog Lake, Ontario. J. Great Lakes Res. 33, 497–504, http://dx.doi.org/10.3394/0380-1330(2007)33[497:TIOTNM]2.0.CO;2.

Holmes, E.E., Lewis, M.A., Banks, J.E., Veit, R.R., 1994. Partial differential equations in ecology: spatial interactions and population dynamics. Ecology 75, 17–29, http://dx.doi.org/10.2307/1939378.

Hussner, A., Stiers, I., Verhofstad, M.J.J.M., Bakker, E.S., Grutters, B.M.C., Haury, J., van Valkenburg, J.L.C.H., Brundu, G., Newman, J., Clayton, J.S., Anderson, L.W.J., Hofstra, D., 2017. Management and control methods of invasive alien freshwater aquatic plants: a review. Aquat. Bot. 136, 112–137, http://dx.doi.org/10.1016/j.aquabot.2016.08.002.

Karst, N., Dralle, D., Thompson, S., 2016. Spiral and rotor patterns produced by fairy ring fungi. PLoS One 11, e0149254, http://dx.doi.org/10.1371/journal.pone.0149254.

Kovalenko, K.E., Thomaz, S.M., Warfe, D.M., 2011. Habitat complexity: approaches and future directions. Hydrobiologia 685, 1–17, http://dx.doi.org/10.1007/s10750-011-0974-z.

Kunii, H., 1982. Life cycle and growth of *Potamogeton crispus* L. in a shallow pond, ojaga-ike. Bot. Mag. Tokyo 95, 109–124, http://dx.doi.org/10.1007/BF02488578.

Leonard, L.A., Croft, A.L., 2006. The effect of standing biomass on flow velocity and turbulence in *Spartina alterniflora* canopies. Estuar. Coast. Shelf Sci. 69, 325–336, http://dx.doi.org/10.1016/j.ecss.2006.05.004.

Leoni, B., Marti, C.L., Forasacco, E., Mattavelli, M., Soler, V., Fumagalli, P., Imberger, J., Rezzonico, S., Garibaldi, L., 2016. The contribution of *Potamogeton crispus* to the phosphorus budget of an urban Shallow lake: Lake Monger, Western Australia. Limnology 17, 175–182, http://dx.doi.org/10.1007/s10201-015-0465-4.

Madsen, J.D., Chambers, P.A., James, W.F., Koch, E.W., Westlake, D.F., 2001. The interaction between water movement, sediment dynamics and submersed macrophytes. Hydrobiologia 444, 71–84, http://dx.doi.org/10.1023/A:1017520800568.

Masselink, G., Pattiaratchi, C.B., Masselinkt, G., Pattiaratchit, C., 2001. Characteristics of the sea breeze system in Perth, Western Australia, and its effect on the nearshore wave climate. J. Coast. Res. 17, 173–187.

Maxwell, P.S., Eklöf, J.S., van Katwijk, M.M., O'Brien, K., de la Torre-Castro, M., Boström, C., Bouma, T.J., Unsworth, R.K.F., van Tussenbroek, B.I., van der Heide, T., 2016. The fundamental role of ecological feedback mechanisms is seagrass ecosystems – a review. Biol. Rev. 92, 1521–1538, http://dx.doi.org/10.1111/brv.12294.

Mazzoleni, S., Bonanomi, G., Giannino, F., Rietkerk, M., Dekker, S.C., Zucconi, F., 2007. Is plant biodiversity driven by decomposition processes? An emerging new theory on plant diversity. Commun. Ecol. 8, 103–109, http://dx.doi.org/10.1556/ComEc.8.2007.1.12.

Mazzoleni, S., Bonanomi, G., Incerti, G., Chiusano, M.L., Termolino, P., Mingo, A., Senatore, M., Giannino, F., Cartenì, F., Rietkerk, M., Lanzotti, V., 2015. Inhibitory and toxic effects of extracellular self-DNA in litter: a mechanism for negative plant-soil feedbacks? New Phytol. 205, 1195–1210, http://dx.doi.org/10.1111/nph.13121.

Meron, E., Yizhaq, H., Gilad, E., 2007. Localized structures in dryland vegetation: forms and functions. Chaos Interdiscip. J. Nonlinear Sci. 17, 37109, http://dx.doi.org/10.1063/1.2767246.

Mitchell, S.F., Hamilton, D.P., Macgibbon, W.S., Nayar, P.K.B., Reynolds, R.N., 1988. Interrelations between phytoplankton, submerged macrophytes, black swans (*Cygnus atratus*) and zooplankton in a shallow New Zealand lake. Int. Rev. Hydrobiol. 73, 145–170, http://dx.doi.org/10.1002/iroh.19880730203.

Muller-Landau, H.C., 2012. Plant Dispersal, In: Encyclopedia of Theoretical Ecology. Univ of California Press, pp. 198–202.

Murphy, E., Ghisalberti, M., Nepf, H., 2007. Model and laboratory study of dispersion in flows with submerged vegetation. Water Resour. Res. 43, W05438, http://dx.doi.org/10.1029/2006WR005229.

Okubo, A., Levin, S.A., 2013. Diffusion and Ecological Problems: Modern Perspectives. Springer Science & Business Media.

Puijalon, S., Bouma, T.J., Van Groenendael, J., Bornette, G., 2008. Clonal plasticity of aquatic plant species submitted to mechanical stress: escape versus resistance strategy. Ann. Bot. 102, 989–996, http://dx.doi.org/10.1093/aob/mcn190.

Pulido, C., Borum, J., 2010. Eelgrass (*Zostera marina*) tolerance to anoxia. J. Exp. Mar. Biol. Ecol. 385, 8–13, http://dx.doi.org/10.1016/j.jembe.2010.01.014.

Qian, C., You, W., Xie, D., Yu, D., 2015. Turion morphological responses to water nutrient concentrations and plant density in the submerged macrophyte *Potamogeton crispus*. Sci. Rep. 4, 7079, http://dx.doi.org/10.1038/srep07079.

Riis, T., Sand-Jensen, K., 2006. Dispersal of plant fragments in small streams. Freshwater Biol. 51, 274–286, http://dx.doi.org/10.1111/j.1365-2427.2005.01496.x.

Riis, T., Madsen, T.V., Sennels, R.S.H., 2009. Regeneration, colonisation and growth rates of allofragments in four common stream plants. Aquat. Bot. 90, 209–212, http://dx.doi.org/10.1016/j.aquabot.2008.08.005.

Riis, T., 2008. Dispersal and colonisation of plants in lowland streams: success rates and bottlenecks. Hydrobiologia 596, 341–351, http://dx.doi.org/10.1007/s10750-007-9107-0.

Rogers, K.H., Breen, C.M., 1980. Growth and reproduction of *Potamogeton crispus* in a South African lake. J. Ecol. 68, 561–571, http://dx.doi.org/10.2307/2259422.

Ruiz-Montoya, L., Lowe, R.J., Kendrick, G.A., 2015. Contemporary connectivity is sustained by wind- and current-driven seed dispersal among seagrass meadows. Mov. Ecol. 3, 9, http://dx.doi.org/10.1186/s40462-015-0034-9.

Ruiz-Reynés, D., Gomila, D., Sintes, T., Hernández-García, E., Marbà, N., Duarte, C.M., 2017. Fairy circle landscapes under the sea. Sci. Adv. 3, e1603262.

Søndergaard, M., Moss, B., 1998. Impact of submerged macrophytes on phytoplankton in shallow freshwater lakes. In: Jeppesen, E., Søndergaard, M., Søndergaard, M., Christoffersen, K. (Eds.), The Structuring Role of Submerged Macrophytes in Lakes. Springer-Verlag, New York, pp. 115–133.

Sand-Jensen, K., Møller, C.L., Borum, J., 2015. High resistance of oligotrophic isoetid plants to oxic and anoxic dark exposure. Freshwater Biol. 60, 1044–1051, http://dx.doi.org/10.1111/fwb.12570.

Sastroutomo, S.S., 1981. Turion formation, dormancy and germination of curly pondweed, *Potamogeton crispus* L. Aquat. Bot. 10, 161–173, http://dx.doi.org/10.1016/0304-3770(81)90018-8.

Sheffer, E., Yizhaq, H., Shachak, M., Meron, E., 2011. Mechanisms of vegetation-ring formation in water-limited systems. J. Theor. Biol. 273, 138–146, http://dx.doi.org/10.1016/j.jtbi.2010.12.028.

Tarnita, C.E., Bonachela, J.A., Sheffer, E., Guyton, J.A., Coverdale, T.C., Long, R.A., Pringle, R.M., 2017. A theoretical foundation for multi-scale regular vegetation patterns. Nature 541, 398–401, http://dx.doi.org/10.1038/nature20801.

Thompson, S., Katul, G., 2009. Secondary seed dispersal and its role in landscape organization. Geophys. Res. Lett. 36, W10421, http://dx.doi.org/10.1029/2008GL036044.

Thompson, S.E., Katul, G.G., 2013. Implications of nonrandom seed abscission and global stilling for migration of wind-dispersed plant species. Glob. Chang. Biol. 19, 1720–1735, http://dx.doi.org/10.1111/gcb.12173.

Umetsu, C.A., Evangelista, H.B.A., Thomaz, S.M., 2012. The colonization, regeneration, and growth rates of macrophytes from fragments: a comparison between exotic and native submerged aquatic species. Aquat. Ecol. 46, 443–449, http://dx.doi.org/10.1007/s10452-012-9413-0.

Ursino, N., 2010. Modeling biomass competition and invasion in a schematic wetland. Water Resour. Res. 46, W08503, http://dx.doi.org/10.1029/2009WR008280.

van der Heide, T., Bouma, T.J., Van Nes, E.H., Van De Koppel, J., Scheffer, M., Roelofs, J.G.M., Van Katwijk, M.M., Smolders, A.J.P., 2010. Spatial self-organized patterning in seagrasses along a depth gradient of an intertidal ecosystem. Ecology 91, 362–369, http://dx.doi.org/10.1890/08-1567.1.

Vári, Á., 2013. Colonisation by fragments in six common aquatic macrophyte species. Fundam. Appl. Limnol. 183, 15–26, http://dx.doi.org/10.1127/1863-9135/2013/0328.

Valley, R.D., Heiskary, S., 2012. Short-term declines in curlyleaf pondweed in Minnesota: potential influences of snowfall. Lake Reserv. Manag. 28, 338–345, http://dx.doi.org/10.1080/07438141.2012.745911.

Verburg, P., Antenucci, J.P., 2010. Persistent unstable atmospheric boundary layer enhances sensible and latent heat loss in a tropical great lake: lake Tanganyika. J. Geophys. Res. 115, D11109, http://dx.doi.org/10.1029/2009JD012839.

Wolfer, S.R., Straile, D., 2004. Spatio-temporal dynamics and plasticity of clonal architecture in *Potamogeton perfoliatus*. Aquat. Bot. 78, 307–318, http://dx.doi.org/10.1016/j.aquabot.2003.11.005.

Wu, J., Cheng, S., Liang, W., He, F., Wu, Z., 2009. Effects of sediment anoxia and light on turion germination and early growth of *Potamogeton crispus*. Hydrobiologia 628, 111–119, http://dx.doi.org/10.1007/s10750-009-9749-1.

Zhou, N., Hu, W., Deng, J., Zhu, J., Xu, W., Liu, X., 2016. The effects of water depth on the growth and reproduction of Potamogeton crispus in an in situ experiment. J. Plant Ecol, rtw048, http://dx.doi.org/10.1093/jpe/rtw048.